Astron. Astrophys. 325, 745–754 (1997)

ASTRONOMY
AND
ASTROPHYSICS

Refined analysis of interplanetary H-Lyα spectra obtained with the Hubble-Space Telescope GHRS spectrometer

Horst Scherer[1], **Hans J. Fahr**[1], **and John T. Clarke**[2]

[1] Institut für Astrophysik und Extraterrestrische Forschung der Universität Bonn, Auf dem Hügel 71, D-53121 Bonn, Germany
[2] Space Physics Research Lab., University of Michigan, Ann Arbor, MI 48109, USA

Received 8 November 1996 / Accepted 17 March 1997

Abstract. Here we present a new synoptic analysis of 5 HST-GHRS interplanetary H-Lyα spectra obtained at different lines of sight from different positions of the earth in its orbit. The spectral analysis aimed at the derivation of actual interstellar gas parameters is carried out on the basis of a newly developed Lyα radiation transport code taking into account the effects of angle-dependent partial frequency redistribution, selfabsorption by the interplanetary hydrogen, and the actual spectral profile of the solar Lyα emission line. As is shown the five different spectra, registered over a total time period of 18 months, when analyzed separately will lead to slightly different LISM parameters, however, if analyzed synoptically can also be reasonably well explained by one common set of LISM parameters. Hereby the fit achieved with the most conventional LISM parameter set (T = 8000 K; v = 26 km/s) can be improved by red-shifting the upwind spectra by -5 km/s. This shift, as we are going to argue, is best explained by a 30°-tilt of the symmetry axis of the heliospheric interface with respect to the LISM helium inflow direction, which could easily be established by LISM magnetic fields of a few μGauss tilted with respect to the helium inflow direction. Enhanced values for the solar Lyα radiation pressure (μ = 1.8) would reduce the needed redshift to less than 2.5 km/s (tilt angles much lower than 30°).

Key words: radiative transfer – interplanetary medium

1. Introduction to problem and motivation

For several decades now attempts have been made to deduce the relevant thermodynamical parameters of the nearby local interstellar medium (LISM) by analyzing interplanetary resonance glow intensities of hydrogen and helium (see e.g. reviews by Fahr 1974; Thomas 1978; Holzer 1977; Bertaux 1984). Up to more recent times these derivations were solely based on frequency-integrated glow intensity data which give added-up contributions from local radiation sources along the line of sight. Thus the interpretation clearly suffers from the fact that hydrogen and helium producing the resonance emission are strongly inhomogeneous along the line of sight that concerns their dynamics and thermodynamics. As one of the consequences one always had to face the puzzling outcome that disjunctive thermodynamical parameters were derived for LISM helium and LISM hydrogen, respectively. Though this difference became more and more accepted as real and as a mere consequence of the interface-filtration suffered exclusively by hydrogen, it was nevertheless hoped all the time for better glow information that could either remove the discrepancies or confirm the interface idea.

This better information is now available in the form of spectrally resolved interplanetary glow data, at least in the case of H-Lyα. The first spectra of the diffuse interplanetary Lyα glow were obtained with the COPERNICUS spectrograph (Adams & Frisch 1977) and with the International Astronomical Explorer (IUE)(Clarke et al. 1984). More recently also the GHRS spectrograph (Goddard High Resolution Spectrograph) of the Hubble Space Telescope (HST) has been used to obtain well resolved interplanetary Lyα emission spectra (Lallement et al. 1993; Clarke et al. 1995; Clarke et al. in prep.). For the analysis of the observed spectra these latter authors have used fits of the spectral data by theoretical spectra generated on the basis of the so-called "classical glow modelling". Within this modelling an optically thin approach is applied to the case of a hydrogen flow over the solar system with homogeneous temperature and a bulk velocity what is allowed to change with position due to net solar potential. Using this approach Lallement et al. (1993) come to the conclusion that the HST-GHRS spectrum, after subtraction of the geocoronal contribution, is best fitted by a model spectrum calculated for hydrogen with an inflow velocity of $V_{H,\infty}$ = 20 km/s. As they can show, at least their fit adopting $V_{H,\infty}$ = 20 km/s is significantly better than their fit taking an inflow of $V_{H,\infty}$ = 26 km/s that is indicated by results of the ULYSSES GAS experiment (Witte et al. 1993), though with an adopted temperature of $T_{H,\infty}$ = 8000 K their modelled profile turns out to be too narrow. With this result the authors conclude that they are seeing the deceleration of the hydrogen flow by about 6 km/s

Send offprint requests to: Horst Scherer

consistent with the charge-exchange-coupling to the interface plasma predicted by Fahr et al. (1986), Fahr (1990), Osterbart & Fahr (1992), Baranov & Malama (1993), or Fahr & Osterbart (1993).

It is the purpose of this paper to show that this conclusion is strongly biased by the "classical spectral modelling" and needs some revision when a more refined spectral analysis is carried out. How much the above conclusion may be biased by the adoption of a homogeneous flow can probably already be deduced from the result of an analogous spectral analysis carried out by Clarke et al. (1984) in which an effective solar gravity field had been admitted operating on hydrogen at its flow over the solar system. If an effective gravity operates on hydrogen, connected with an effective solar mass $M_{eff} = (1- \mu)\ M_o$, then the hydrogen bulk velocity locally varies, i.e. is inhomogeneous. Then a part of the spectral spread cannot be interpreted as due to thermal motions, but is caused by the bulk velocity spread along the line of sight. An interesting hint to the effect of this bulk velocity spread is the fact that Clarke et al. (1984) using $\mu = 0.8$ (instead of $\mu = 1$, as taken by Lallement et al. 1993) derive an LISM hydrogen inflow velocity of $V_{H,\infty} = 25.6$ km/s, a value which is fairly close to that obtained by Witte et al. (1993) for LISM helium. In addition in the analysis of Lallement et al. (1993) and Clarke et al. (1984, 1995) no interface effect was consistently and implicitly taken into account in the modelling of the interplanetary hydrogen distribution. If this effect is taken into account in a kinetic form (Osterbart & Fahr 1992; Baranov & Malama 1993), then in fact a deceleration of the hydrogen bulk flow occurs in the upwind region at large solar distances of about 80 to 100 AU. Closer to the sun, where the radiation sources for the HST-GHRS spectrum are located, no deceleration is left, in contrast here even enhanced bulk velocities arise. Thus one may doubt whether from a spectral analysis using an inconsistent inclusion of the interface, the flow deceleration by the interface can be identified. We thus feel that a refined analysis of GHRS-HST interplanetary Lyα spectra is needed in order to arrive at more solid LISM parameter and interface derivations. In the analysis which we present in this paper we shall start out from interface-modulated hydrogen distribution functions and shall include the case of effective solar gravity (i.e. $\mu \neq 1$). Furthermore we use a newly developed radiation transport code to calculate the Lyα spectra in which we take into account the actual solar emission profile, self-absorption of the interplanetary hydrogen, and angle-dependent partial frequency redistribution.

2. Method and description of the observations

We have obtained observations of spectral Lyα emission from five different directions at five positions of the earth in its orbit. The spectral observations were carried out with the GHRS, echelle A, spectrograph on-board the Hubble Space Telescope using the large science aperture (LSA) at 1216 Å. Meanwhile it has become clear that the GHRS Echelle A spectra are more than sufficient to resolve the velocity structure in the interplanetary hydrogen flow at a satisfactory signal/noise level (see Clarke et al. 1995). These spectra by their specific profiles in different line-of-sight directions thus are the key to distinguish between authentically solar effects and interface effects modulating the dynamics of hydrogen in the heliosphere. The nature of the point spread function (PSF) for diffuse monochromatic emission has already been examined in some detail (Clarke et al. 1995). For this purpose the scattering wings and the occurrence of grating ghosts within a few Å of the line center have to be taken into account. The general characteristics of the GHRS gratings are reported by Cardelli et al. (1990, 1993), and the data given there are applicable to point source observations. When observing diffuse emission the resulting PSF then can be synthesized as the sum of point sources filling each of the eight diodes corresponding to the 2 arcsec aperture. The result of this synthesis is a nearly rectangular PSF with a full width half maximum of 0.07 Å and a scattered light level in the wings larger by the ratio of increased area of the emission region in the aperture. Here the large aperture was required to obtain a sufficient level of signal-to-noise.

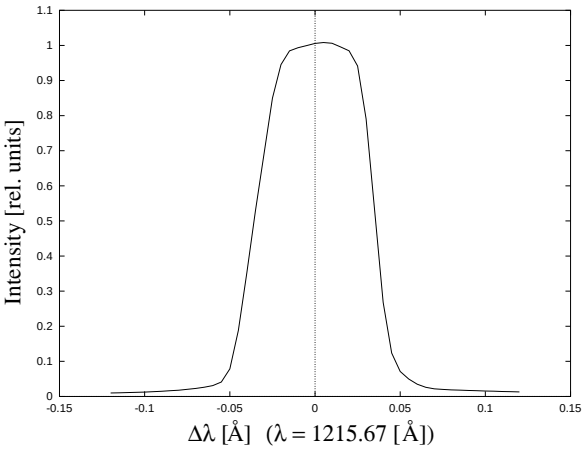

Fig. 1. Point Spread Function of the HST GHRS instrument (from Clarke et al. 1995).

3. Brief description of the observations

Till now there exist 5 HST spectral intensity measurements of the interplanetary hydrogen H-Lyα resonance glow at 5 different targets taken at 5 different times (see Table 1). The data are high resolution registrations from 1212.3 Å to 1218.7 Å measured by the GHRS on board the HST during extended exposure time periods.

The surveys were made in the 'FP-SPLIT' mode of the GHRS instrument. For every position and view direction, where H-Lyα data are available, between 4 and 10 data sets exist, with an integration time of 544 sec each (with few exceptions of shorter integration times). With appropriate IDL-software procedures these data sets belonging to one target will all be merged resulting in noise-reduced spectra for every view direction. (Details of the GHRS instrument and data handling ('FP-SPLIT' mode) in Baum (1994), or Soderblom (1994)).

Table 1. HST measurement data

Nr.	date	pos. of earth ($\beta \equiv 0^o$)	v direction of earth ($\beta \equiv 0^o$)	line of sight	v rel. LOS
1	07.04.94	λ= 17.15 ^{o}	λ = 107.15 ^{o}	λ = 253.23 ^{o} β = 7.01 ^{o}	-24.71 kms^{-1}
2	04.06.94	λ= 74.32 ^{o}	λ = 164.32 ^{o}	λ = 165.96 ^{o} β = -5.64 ^{o}	29.84 kms^{-1}
3	06.03.95	λ= 346.22 ^{o}	λ = 76.22 ^{o}	λ = 72.61 ^{o} β = -5.19 ^{o}	29.82 kms^{-1}
4	25.03.95	λ= 4.74 ^{o}	λ = 94.74 ^{o}	λ = 253.23 ^{o} β = 7.01 ^{o}	-27.70 kms^{-1}
5	09.03.96	λ= 349.18 ^{o}	λ = 79.18 ^{o}	λ = 72.61 ^{o} β = -5.19 ^{o}	29.68 kms^{-1}

3.1. The Doppler shift

The HST is an earth-bound satellite, thus, all data are strongly influenced by the Doppler shift caused by both the HST orbital motion with respect to the earth and of the ecliptical motion of the earth around the sun. The velocity components of these motions relative to the line of sight (LOS) have to be taken into account when comparing the data with theoretical radiative transport calculations (Sect. 4).

3.1.1. The HST orbital motion

In all measured data the geocoronal H-Lyα glow, as the strongest spectral feature, is seen (Fig. 6). Assuming that the earth's atmosphere is fixed to the earth, the Doppler shift along LOS caused by the HST orbital motion around the earth is identical for the geocorona and the interplanetary H-Lyα glow. By determining the shift of the geocoronal spectra measured by the GHRS with respect to geocoronal rest frame and by a corresponding shift of the data, the influence of the HST orbital motion on the spectral location of the interplanetary H-Lyα glow data are eliminated. (Barycentric motion moon-earth only plays a minor role and will be neglected).

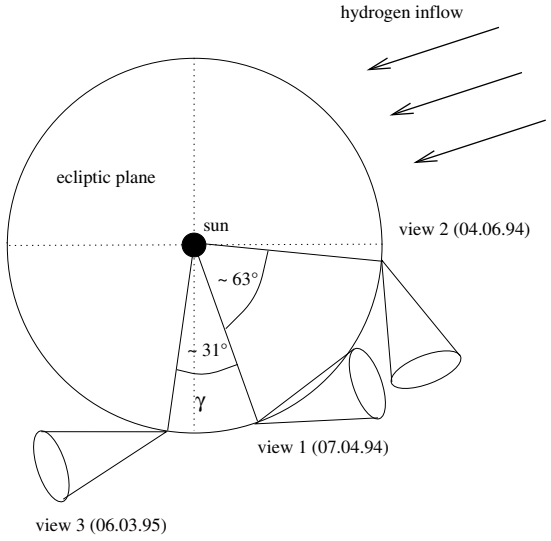

Fig. 2. Position and view direction of the GHRS HST instrument. (note: view 4 $\sim$ view 1, view 5 $\sim$ view 3, see Table 1). The hydrogen inflow direction is adopted with α = 253.5^o and $\delta = -15.5^o$ (Lallement et al. 1993)

3.1.2. The ecliptical motion of the earth

For each day for which HST data were available the earth's velocity vector was obtained by taking the derivatives of the J2000 ephemeris coordinates; the Earth-Moon motion and the sun-barycenter motion have not been taken into account. The resulting velocity vector has an accuracy of 0.025 km/s within the epoch range of 1900 to 2100 AD. Transforming the earth's velocity vector and the GHRS instrument view direction in cartesian coordinates for every day of measurement, the earth velocity component into the LOS direction is given by the scalar product of these two vectors (see Table 1).

The remaining shift of the H-Lyα background glow is caused by the ("Doppler-shift" projection of the) velocity pattern of the interplanetary hydrogen to the GHRS line of sight and is taken into account by the radiation transport model (Sect. 4).

3.2. The GHRS instrument function

The instrument point spread function (PSF) of the GHRS describes how an actual monochromatic point source is spectrally broadened by the electrical and optical instrument environment and by the optical slit-spectrometer mounting. This instrument function has been determined by several authors (e.g.: Clarke et al. 1995; Gilliland et al. 1992) (Fig. 1).

Because the real observational data are very noisy, it is not advised here to deconvolve the data from this PSF. Instead it is more convenient to convolve the model results with this PSF and compare these results with the data (Sect. 6). The calculated spectra (Sect. 4) are similar to a Voigt profile with a temperature of the order of 10000^o K. After the convolution of the calculated spectra with the GHRS PSF function (with $\sim$ 0.1 Å, see Fig. 1) the resulting spectra are then like a Voigt profile with a temperature of 30000 ^{o} K (see Fig. 5).

4. The Lyα radiation transport code

The variation of H-Lyα resonance emission intensity with the line element counted along the line of sight in an emitting and reabsorbing interplanetary H-medium is determined by loss and gain processes of photons and is given by the well-known radiation transport equation. This equation is an integro-differential equation which usually is treated by introducing the optical depth τ (e.g. Mihalas 1978). The formal solution of the radiation transport equation can be obtained in the form of a Neumann

series expansion (Courant & Hilbert 1968) with respect to scattering orders i, leading to the following representation (Fahr & Smid 1982, Fahr et al. 1986, Scherer & Fahr 1996).

$$I = \sum_i I_i \tag{1}$$

with

$$I_i(\tau, \mathbf{\Omega}, \nu) = \int_{\tau(r_0)}^{\tau(r)} \frac{1}{4\pi} \int_{\nu'} \int_{\mathbf{\Omega}'} I_{i-1}(\tau', \mathbf{\Omega}', \nu') R(\mathbf{\Omega}', \nu', \mathbf{\Omega}, \nu) \mathrm{d}\mathbf{\Omega}\, \mathrm{d}\tau' \mathrm{d}\nu' \tag{2}$$

If the intensity I_o of the primary source (here the sun) is known, all higher scattering orders (I_1 to I_n) at any position in space successively can be determined with the above equation. $R(\Omega', \nu', \Omega, \nu)$ is the angle-dependent, partial redistribution function and describes the probability that a photon within the original frequency interval $\nu' + \mathrm{d}\nu'$ arriving from the solid angle $\Omega' + \mathrm{d}\Omega'$ will be absorbed and will be re-emitted within the frequency interval $\nu + \mathrm{d}\nu$ into the solid angle $\Omega' + \mathrm{d}\Omega'$ (see Hummer 1962, modified by Scherer & Fahr 1996).

For a solution of Eq. (1) and Eq. (2) one has to start from the sun as the central source of the H-Lyα radiation and to use the thermodynamical conditions of the interplanetary hydrogen to specify the redistribution function (Scherer & Fahr 1996). Based on the analytical and numerical concept for solving the first and second order of Eq.(2), it can be shown that the second and all higher scattering orders only play a minor role for intensities registered at solar distances smaller than 5 AU when taking into account the actual local temperature and velocity of the hydrogen, and also the angle- and frequency- dependence of photon redistribution by the the scattering agent (Scherer & Fahr 1996).

In this case equation (Eq. 1) can then be approximated by

$$I = \sum_i I_i \sim I_1 = I_S \tag{3}$$

and one finally obtains for I_S (Details in Scherer & Fahr 1996)

$$\begin{aligned} I_S(\boldsymbol{r}, \Omega_{view}, \nu) = {} & I_\odot\, k_0 \int_{\rho'} \int_{\nu'} n\left(\boldsymbol{r}_L(\rho')\right) \frac{r_E^2}{\boldsymbol{r}_L^2(\rho')} \\ & \left(A e^{\left(-\frac{(\nu'-\nu_0)^2}{\Delta\nu_A^2}\right)} - B e^{\left(-\frac{(\nu'-\nu_0)^2}{\Delta\nu_B^2}\right)} \right) \\ & R\left(\boldsymbol{n}_S(\boldsymbol{r}_L(\rho')), \nu', \boldsymbol{n}(\Omega_{view}), \nu, \boldsymbol{v}_0(\boldsymbol{r}_L(\rho')), T_{H_r}(\boldsymbol{r}_L(\rho'))\right) \\ & \exp\left[- \int_0^{\boldsymbol{r}_L(\rho')} k(\nu', T_{H_r}(\boldsymbol{r})) n(\boldsymbol{r})\, ds \right] \\ & \exp\left[\int_{\rho'}^{0} k(\nu, T_{H_r}(\boldsymbol{r}_L(\rho'')) n\left(\boldsymbol{r}_L(\rho'')\right)\, d\rho'' \right] d\nu'\, d\rho' \end{aligned} \tag{4}$$

In this equation $I_\odot$ represents the total H-Lyα flux of the solar disk, k_0 the H-Lyα absorption cross section of hydrogen, $A, B, \Delta\nu_A, \Delta\nu_B$ are the appropriate parameter of a fit to the solar H-Lyα emission line, $\boldsymbol{v}_0(\boldsymbol{r}), T_{H_r}(\boldsymbol{r}), n(\boldsymbol{r})$ are local quantities of the bulk velocity, radial temperature pattern and density distribution of the interplanetary hydrogen and $\boldsymbol{r}_L(\rho)$ is the parametrized line of sight for a detector at a given position $\boldsymbol{r}$ with a view direction $\mathbf{\Omega}$ in space.

All remaining integrations in Eq. 4 have to be done numerically with the use of a theoretical model description of the interplanetary hydrogen distribution developed by Osterbart & Fahr (1992), Fahr & Osterbart (1993,1995), (see below) and as result of these scattering calculations we obtain a specific spectrum for every position and viewing direction of the probe.

4.1. The density model by Osterbart and Fahr

Based on the Parker model (Parker 1963), used for the description of the heliospheric flows, Osterbart & Fahr (1992) use a gas kinetic approach by means of the Boltzmann equation to describe the heliospheric hydrogen distribution. In this approach they take into account the charge exchange processes of the hydrogen with the interface plasma. They determine the time-independent distribution function $f(\boldsymbol{r}, \boldsymbol{v})$ of the interplanetary hydrogen in the vicinity of the sun. Assuming a rotation symmetry with respect to the inflow direction of the interstellar medium, i.e.: f depends only on the radial solar distance r, the angle θ (measured against the inflow direction of the hydrogen) and the local velocity vector, meaning:

$$f(\boldsymbol{r}, \boldsymbol{v}) = f(r, \vartheta, \boldsymbol{v}) \quad ; \quad \boldsymbol{r} = (r, \vartheta, \phi) \tag{5}$$

The earlier model by Osterbart & Fahr (1992) was recently modified by Kausch (1996). Within this refined and improved model it is possible to consider variable ratios of radiation force to gravitation force ($\equiv \mu$) especially important in the vicinity of the sun and needed for the reliable theoretical description of the GHRS HST H-Lyα glow data.

By calculating the higher moments of the distribution function the density, velocity and temperature pattern of the interstellar hydrogen in the neighborhood of the sun is derived (Fig. 3).

$$n_H(\boldsymbol{r}) = \int d^3v f_H(\boldsymbol{r}, \boldsymbol{v}) \tag{6}$$

$$\boldsymbol{u}_H(\boldsymbol{r}) = \frac{1}{n_H(\boldsymbol{r})} \int d^3v \boldsymbol{v} f_H(\boldsymbol{r}, \boldsymbol{v}) \tag{7}$$

$$T_H(\boldsymbol{r}) = \frac{1}{n_H(\boldsymbol{r})} \int d^3v \frac{m(\boldsymbol{v} - \boldsymbol{u}_H(\boldsymbol{r}))^2}{3k} f_H(\boldsymbol{r}, \boldsymbol{v}) \tag{8}$$

The parameters of the interstellar hydrogen used here in the density model are: density $n_\infty = 0.05\ \mathrm{cm}^{-3}$, temperature $T_\infty = 8000$ K, inflow velocity $v_\infty = 26\ \mathrm{kms}^{-1}$ and a termination shock located at 80 AU (more details in Osterbart & Fahr (1992)).

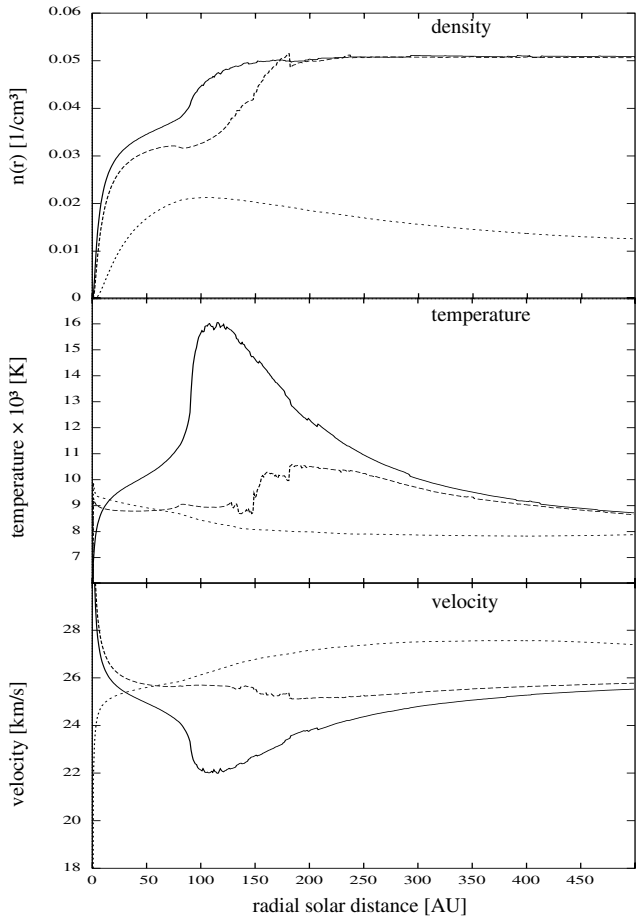

Fig. 3. Local density, temperature and bulk velocity (axial component) values for $\mu = 0.7$ derived with the density model by Osterbart & Fahr are shown as function of radial solar distance for three different angles θ i.e.: – $\theta = 0^o$; - - - $\theta = 90^o$; - - - $\theta = 180^o$.

In Fig. 3 one sees a deceleration of the hydrogen at around ~ 130 AU, i.e. the assumed termination shock. Inside the termination shock especially the slower moving hydrogen atoms are influenced by the solar wind. For passing a given distance slower moving atoms need more time than faster moving atoms. Although the ionisation cross section for hydrogen is only weakly dependent on the relevant velocities, a larger proportion of the slower-moving hydrogen is ionized than of the faster-moving hydrogen, because for equal distances covered, the former is affected by the solar wind for a longer time than the latter. Therefore, in the vicinity of the sun the low-velocity wing of the hydrogen distribution function is decreased in comparison to the high-velocity wing of the distribution function. So, the mean weighted value for the bulk velocity is shifted to higher values. This means that near the sun the bulk velocity evidently increases, and nothing is left of the deceleration of hydrogen seen at regions close to the shock.

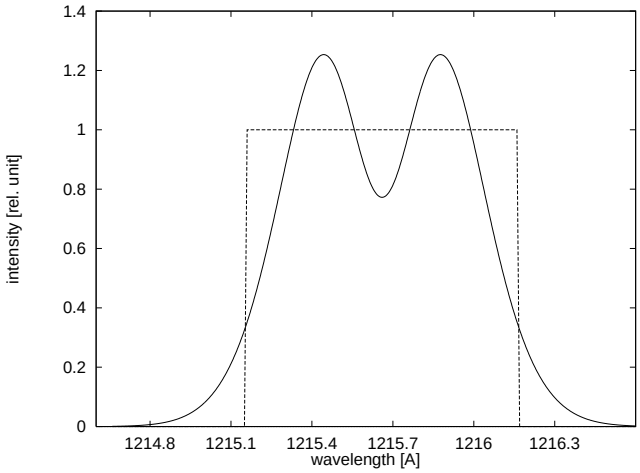

Fig. 4. Different solar Lyα emission profiles alternatively used in the radiation transport model by Scherer & Fahr (1996) and also used here.

5. Results of the theoretical approach

For the purpose of a comparison with earlier spectral calculations of this type (e.g. Lallement et al. 1993, Clarke et al. 1995) and for the sake of identifying clearly the deviations from our present improved and more sophisticated calculations, we show theoretical results for two different cases:

1. the radiation transport model was used
   a. adopting a flat solar profile (Fig. 4)
   b. not taking into account the optical depth (optically thin approximation)
   c. using an "interface"-free density model that results from the model by Osterbart & Fahr (1992) if the LISM-plasma density vanishes, nearly identical with the density model by Wu & Judge (1979) for an effective solar gravity of $\mu = 1$ (see Sect. 1).

2. the radiation transport model (Scherer & Fahr 1996) was used
   a. adopting a realistic solar profile (Fig. 4), resulting by a fit to OSO 8 satellite data Bonnet et al. (1978)
   b. taking into account the optical depth
   c. using a density model taking into account the interface effect, assuming a shock position at 80 AU solar distance and an effective solar gravity of $\mu = 0.7$ (see Sect. 1).

The solar profiles used in the above cases are scaled such that in both cases the area under the curves is equal to unity (see Fig. 4).

In addition in Fig. 5 a Voigt-profile with an assumed temperature of 30000 K is shown as it was used by Clarke et al. (1995) or Lallement et al. (1993). This Voigt-profile is the result of a best fit procedure to the HST data. The maximum of the Voigt-profile is rescaled and shifted, so that its maximum is identical with that of the spectrum calculated with the radiation transport model (case 2).

Between the spectra of case 1 and case 2 there are some remarkable differences evident. The upwind spectra of case 2

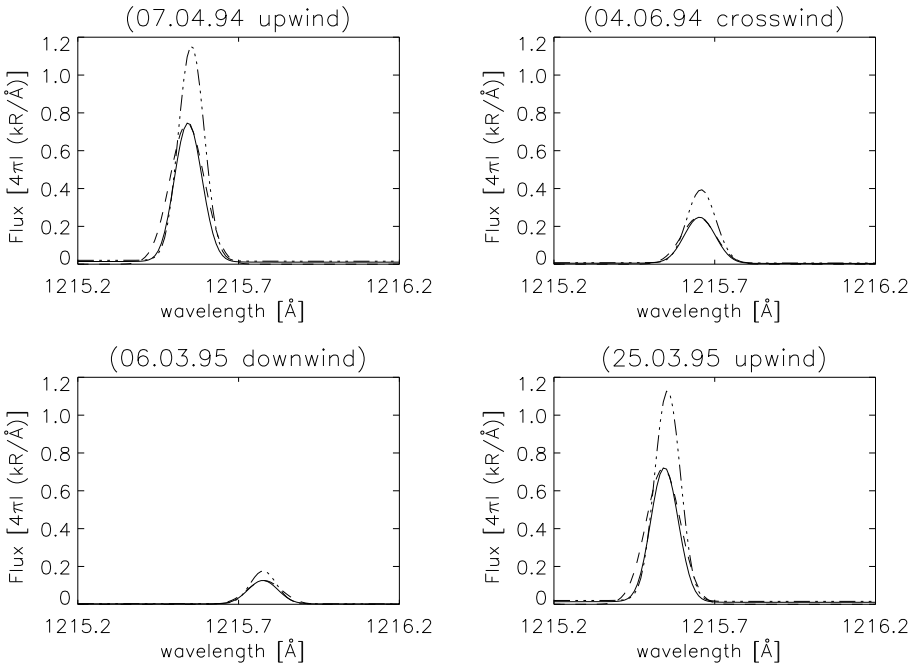

Fig. 5. Calculated spectra for alternative assumptions: - - - Voigt-profile with 30000 K; case 1: - · · · - radiation transport model by Scherer & Fahr using a flat solar profile and an optically thin approximation (details see text). case 2: – radiation transport model by Scherer & Fahr using a realistic solar profile, angle-dependent redistribution and selfabsorption. The different cases are calculated for the four positions and view directions of the HST (see Table 1).

are shifted a little bit towards the blue spectral wings. This is caused mainly by the different effective solar gravity used in the different density models. For $\mu = 0.7$ an attracting gravitational potential operates in the vicinity of the sun which speeds up the neutral hydrogen, and its resonant $H_{Ly\alpha}$ glow is shifted by the Doppler effect to shorter wavelengths when looking upwind. The opposite relation exists in the downwind direction. Due to the differential depletion of the hydrogen velocity distribution function, the downwind hydrogen glow spectra are shifted by the Doppler effect to longer wavelengths when an attracting solar gravitational potential exists. The different intensities of case 1 and case 2 are caused by the different hydrogen distributions of the density models and the different solar profiles. The influence of the different solar profiles is more clearly seen in calculations of complete sky surveys (see Scherer & Fahr 1995, 1997).

Re-scaling the spectra of case 1 and case 2 to the same maximum shows that the spectra of case 2 are relatively broader than the spectra of case 1. In case 2, caused by the effective solar gravity, the neutral hydrogen distribution for off axis hydrogen atoms has velocity components perpendicular to the inflow direction. This perpendicular velocity components broaden the hydrogen distribution function in velocity-space and, caused by the Doppler effect, the theoretical backscattering $H_{Ly\alpha}$ glow spectra also are broadened. The maximum of the case 2 spectrum is lower due to the different solar profiles used by the calculation of case 1 and case 2 (Fig. 4). In a comparison of the theoretical results with the HST data only the widths and spectral location of the maximum of the spectra are important, because the absolute, time-variable solar $H_{Ly\alpha}$ intensity (solar cycle, etc.) influencing the absolute glow intensities at the event of observation is unknown. In case it would be known for the moment of observation also the absolute value of the HST spectral intensities could be used for H-density determinations. This is why the theoretical results have to be rescaled for comparison with the HST data (see Sect. 6).

The Voigt-profile with 30000 K, resulting by a best fit to the HST data (Clarke et al. 1995) is broader than calculations for the case 2 of the radiation transport model by Scherer & Fahr (Fig. 5). As an explanation we may offer the following reason: the radiation transport model assumes a sharp line of sight in the numerical procedure whereas in reality HST GHRS instrument has a cone with finite opening angle. Therefore, by not taking into account the actual aperture of the HST instrument the line width, calculated with the radiation transport model, underestimates the line width by a small amount.

6. Comparison the HST-GHRS spectral data with theoretical calculations

From the comparison of different theoretical calculations concerning expected Lyα spectra shown in Fig. 5 one can easily conclude that the different ingredients entering the calculations in case 1 and case 2 can definitely influence the values of LISM parameters best fitting the actual, observational HST results. Compared to case 2 (realistic solar profile, self-absorption, active interface), in case 1 (flat solar profile, no self-absorption, no interface) one derives spectral features with smaller blue shifts for the upwind and crosswind spectra and with substantially higher spectral peak intensities though starting from identical LISM parameters. From this experience it turns out that for a reliable parameter analysis based on comparisons of data with theory one has to include effects only appropriately taken into account by case 2 of our calculations. In the following spectral analysis we therefore start out from "case 2" calculations (i.e. actual solar Lyα emission profile, interplanetary self-absorption,

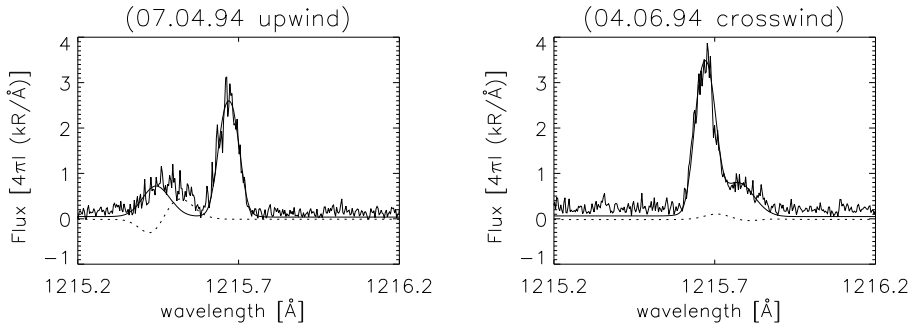

Fig. 6. Comparison of the HST data with the theoretical result (case 2). – calculated spectrum by the radiation transport model by Scherer & Fahr using a realistic solar profile; · · · · · · difference of best data fit and calculated intensity (I_{fit} - I_{theo}) see text.

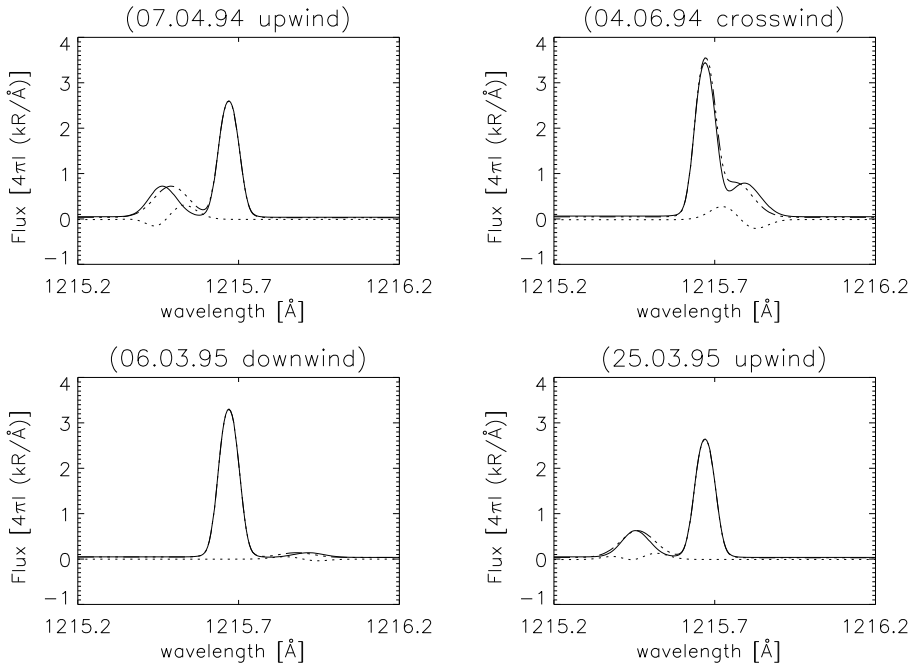

Fig. 7. -· · -Voigt-profile of 30000 K (best fit to the HST data). – calculated spectrum (radiation transport model by Scherer & Fahr, red-shifted by 0.02 Å). · · · · · · difference of best data fit and calculated intensity (I_{fit} - I_{theo}) see text.

heliospheric interface effect is taken into account) for a definite set of LISM parameters (see Tab. 1).

In Fig. 6 we show HST-GHRS spectra and theoretical spectra obtained by the case-2 calculations described in this paper for a set of LISM parameters mentioned in table 1. Although for the set of adopted LISM parameters the calculated spectra fit the data fairly well, one may nevertheless notice spectral regions where data and theory clearly deviate from each other. In order to clearly identify such regions in Fig. 6 where deviations become manifest we have also plotted the differences (I_{fit} - I_{theo}) as function of the wavelength. (I_{fit} is the best fit result to the HST data applying a Voigt-profile of 30000 K, see Clarke et al. (in prep.)). Though it can be seen that these differences are always smaller than the intensities, especially in the 94-upwind spectrum (Fig. 6a) one may notice non-negligible deviations which seem especially due to the fact that the theoretical spectrum is too much blue-shifted with respect to the data.

To improve on this fact we have tested how an artificial red-shift of the theoretical spectrum by 0.02 A (Fig. 7) (corresponding to a bulk velocity decrease by $\sim$ 5.0 km/s, respectively) would reduce the resulting intensity differences. It can be seen when comparing Figs. 6 and 7 that a red-shift by 5 km/s would

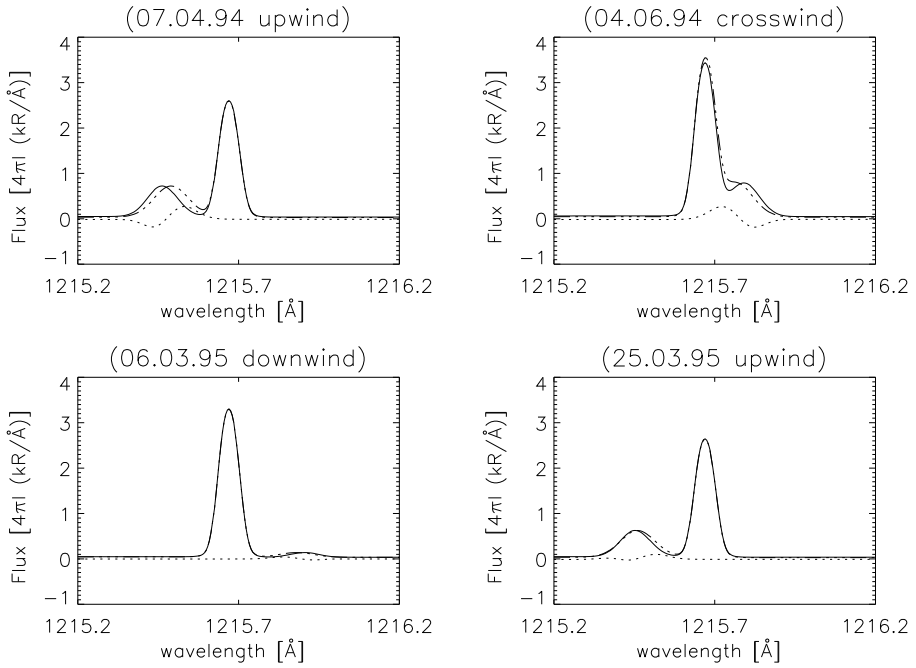

Fig. 8. -·· ·- Voigt-profile of 30000 K (best fit to the HST data). – calculated spectrum (radiation transport model by Scherer & Fahr, using a density model with μ = 1.8). · · · · · · difference of best data fit and calculated intensity (I_{fit} - I_{theo})

lead to definitely better fits for the upwind spectra while larger shifts would again increase the resulting differences. For the crosswind spectrum the unshifted theoretical spectrum shows the smallest deviation between the data and the calculated spectrum i.e. a general shift does not improve the synoptic fit of all spectra. As we can show, there is much less need for a redshifting of the calculated spectra if larger values for the solar Lyα radiation pressure are adopted for the period of the HST-observations. Taking a value of μ = 1.8 which could easily be justified on the basis of the SME satellite measurements (Rottman 1988) or the SOLSTICE-measurements (Rottman et al. 1994; White et al. 1994) one would be left only with a redshift need corresponding to < 2.5 km/s (Fig. 8). However, high values for μ can only be expected at near solar maximum, while for the period of our HST-observations (1994, 1995) definitely lower values must be expected.

The downwind spectra (spectrum from 09.03.96) not shown here, but very similar to the spectrum from 06.03.95 Fig. 6 have a very low significance level (i.e too few statistics). Thus no reliable fits for determining width and position of the interplanetary Lyα spectrum could be done for these two downwind data sets of the HST. Though in these spectra a clear signature of the Lyα glow is seen, they can hardly be used for interpretation purposes (see below).

7. Conclusion

In the afore going section we have shown that there exists some discrepancy between the HST H-Lyα glow data and the theoretical approach. The widths of the theoretical spectra calculated with our radiation transport model are slightly smaller than the measured HST spectra. This problem is mainly caused by not taking into account the actual aperture of HST GHRS instrument and by using a simplified method in correcting for the Doppler shift due to the earth's motion in the ecliptic plane e.g. not taking into account sun-barycenter motion, earth-moon motion (see Sect. 3). Taking these effects into account needs much more work on the data what is not worth the effort because the uncertainties (noise) in the present HST-data are of comparable order.

The discrepancy, however, between the interplanetary hydrogen inflow velocity, determined with the HST spectra and the theoretical spectra, is not explained by an uncertainty in the data. The only uncertainty in deriving the hydrogen inflow velocity from the HST data is caused by a simplified calculation of the earth's velocity component along the detectors' line of sight (Sect. 3.1.2). This amounts to the order of 0.025 km/s. As we see in Fig. 7 a red-shift of the calculated upwind spectra by $\sim$ 5 km/s, much higher than the admittable uncertainty of 0.025 km/s, decreases the difference between data and theoretical spectra. The HST upwind spectra would imply a hydrogen inflow velocity of $\sim$ 21 km/s which is in a clear contradiction to inflow velocity measurements of the LISM helium by the ULYSSES GAS experiment (Witte et al. 1993). The ULYSSES GAS experiment indicates a LISM helium inflow velocity of 26 km/s and, assuming a dynamical equilibrium in the LISM plasma far away from the sun, the same inflow velocity of 26 km/s should be valid for LISM hydrogen. Also the theoretical description of the crosswind spectrum, best fitted with no redshift at all, becomes worse for lowering the hydrogen inflow velocity.

Several authors (e.g. Lallement et al. 1993) tried to explain this velocity discrepancy with the hydrogen deceleration at the LISM interface. In fact close to the shock region at about 80 - 100 AU in the upwind direction the density models (e.g. Osterbart & Fahr 1992; Baranov & Malama 1993) predict such an

effect for hydrogen (see Fig. 3). But taking this interface effect into account in a kinetic form, as is done by the density models used here, in the vicinity of the sun, where the majority of the H-Lyα sources seen by the HST GHRS instrument are located, no deceleration is left. The deceleration results from the fact of a different charge-exchange influence to the different parts of the H-velocity distribution function. It should not be identified with the action of a force. So only decreasing the hydrogen inflow velocity at infinity, would improve the theoretical description of the HST data, but this implies, as mentioned before, the HST data are in contradiction to the ULYSSES GAS experiment. Also the discrepancy of the HST crosswind spectrum is not resolved, since the best theoretical description is given by the unshifted case, and the theoretical spectrum becomes worse for lowering the hydrogen inflow velocity at infinity. Also the crosswind spectrum is affected by such a shift since the projection of the relative velocity of the earth-bound HST to the line of sight counts for the spectral shift.

We have mentioned the remarkable fact that Doppler redshifts of the calculated upwind spectra by equivalent velocities of about -5 km/s noticeably improve the fits to the observed HST-spectra while with this procedure practically no improvement is achieved for the crosswind spectrum. As we could clearly rule out, a change of the actual ionisation rate within supportable limits is no remedy for this flaw in the theoretical representation either. Due to a change in the differential extinction of the hydrogen velocity distribution function a change in the effective bulk velocity will occur. However, the admitted magnitude of this change is much less than 5 km/s. Understanding this improvement in the upwind spectral fits as a serious hint to a needed correction in the modelled hydrogen dynamics one would have to ask how a decelerated hydrogen flow could be achieved in the upwind direction at solar distances that contribute to the HST-spectra. Since the distances of HST-relevant Lyα scattering sources are between 1 and 5 AU one should find an explanation for a decelerated flow at these distances. Though all interface models presented in the literature up to now can predict interface-induced hydrogen deceleration of the order of 5 km/s at large distances (> 60 AU), no deceleration are pointed out by these models for much smaller distances. Here one could only have a hydrogen flow decelerated by 5 km/s if it were already decelerated by this amount far ahead of the interface region, meaning that LISM hydrogen and helium should be dynamically de-coupled. Since this conclusion because of many physical reasons is hard to accept, we here thought of two alternative reasons why upwind hydrogen could appear decelerated at regions close to the sun (1 to 5 AU).

a) This could be due to anomalously large values of the solar Lyα radiation pressure like given by $\mu \geq 1.8$ (see Fig. 8) (unlikely as mentioned before) or even:

b) This could be since the "expected" upwind direction for hydrogen is not coincident with the LISM helium inflow direction but is tilted with respect to that by an angle ϕ such that the projected Doppler velocity thereby becomes smaller by about 5 km/s. With simple algebra one calculates that a tilt angle: ϕ = arccos (21/26) = 36^o: would actually cover the needs. The following physical condition can be envisioned: Assume the solar system to be moving with 26 km/s into a direction characterized by the unit vector $\boldsymbol{n}_{\rm up}$. The LISM magnetic field $\boldsymbol{B}_{\rm LISM}$ may be inclined to this direction by an angle θ given by: $\cos(\theta) = \frac{\boldsymbol{n}_{\rm up} \cdot \boldsymbol{B}_{\rm LISM}}{\|\boldsymbol{B}_{\rm LISM}\|}$. Then a squeezed interface structure will be established as the result of magnetohydrodynamic stress forces (see Fahr et al. 1988). The resulting interface has a symmetry axis which is tilted by $\phi \neq \theta$ with respect to $\boldsymbol{n}_{\rm up}$. While helium not coupling to this squeezed interface will still enter the solar system from the direction $-\boldsymbol{n}_{\rm up}$, hydrogen has to attain the imprint of this interface. Thus, if LISM hydrogen entering from the left side of $\boldsymbol{n}_{\rm up}$ is more extinguished than that entering from the right side, this evidently then leads to a tilt of the hydrogen inflow direction towards the right side. The needed tilt of the interface axis with respect to the helium inflow could easily occur if magnetic fields of the order of a few μGauss are present in the LISM which are tilted by some angle with respect to the plasma bulk flow or LISM helium flow vector. The exact conditions for such tilted magnetic interfaces are analyzed in a paper by Fahr et al. (1988). The needed tilt angle of $\phi = 36^o$ which may be indicated from the above spectral fit procedures can then be interpreted in terms of LISM magnetic field inclinations and magnitudes needed. Recently Ratkiewicz et al. (1996) have published results on 2-D MHD simulation of the heliospheric interface configuration which even allow quantitative conclusions with this respect.

Acknowledgements. This work is based on observations with the NASA/ESA Hubble Space Telescope, obtained at the Space Telescope Science Institute, which is operated by the AURA, Inc. for NASA under contract NSA5-26555. The research was supported by University of Michigan.

References

Adams T.F., Frisch P.C., 1977, ApJ 212, 300
Baum S., 1994, HST Data Handbook, Version 1.0 (Space Telescope Science Institute Baltimore, Maryland)
Baranov V.B., Malama Yu.G., 1993, JGR 98, 157
Bertaux J.L., 1984, Local Interstellar medium, IAU Colloquium No. 81, ed. Y.Kondo, F.C.Bruhweiler, B.D.Savage (NASA cp2345)
Bonnet R.M., Lemaire P., Vial J.C., et al., 1978, ApJ 221, 1032
Cardelli J.A., Ebbets D.C., Savage B.D., 1990, ApJ 365, 789
Cardelli J.A., Ebbets D.C., Savage B.D., 1993, ApJ 413, 401
Clarke J.T., Bowyer S., Fahr H.J., Lay G., 1984, A&A 139, 389
Clarke J.T., Lallement R., Bertaux J.-L., Quemerais E., 1995, ApJ 448, 893
Courant J.T., Hilbert R., 1968, Methoden der mathematischen Physik I, Springer; Berlin, Heidelberg, New York
Fahr H.J., 1974, Space Sci. Rev. 15, 483
Fahr H.J., Smid T., 1982, JGR 87, 2487
Fahr H.J., Lay G., Smid T., 1986, Annales Geophysicae 4A, 447
Fahr H.J., Grzedzielski S., Ratkiewicz R., 1988, Annales Geophysicae 6(4), 337
Fahr H.J., 1990, in: 1. COSPAR Colloquium (Warsaw, Poland) on "Physics of the Outer Heliosphere", Page E, Grzedzielski S. (eds.). Pergamon Press, Oxford, p. 327
Fahr H.J. Osterbart R., 1993, Advances in Space Res. 13(6), 159
Fahr H.J., Osterbart R., 1995, Advances in Space Res. 16(9), 125

Gilliland R.L., Morris S.L., Weymann R.J., Ebbets D.C., Lindler D.J., 1992, PASP 104, 367
Holzer E.T., 1977, ARA&A 27, 199
Hummer D.G., 1962, MNRAS 125, 21
Kausch T., 1996, Das Heliosphärenplasma unter Einfluß von Pickup-Ionen und moduliertem Sonnenwindschock, Diploma thesis (June 1996), Univ. of Bonn
Lallement R., Bertaux J.L., Clarke J.T., 1993, Science 260, 1095
Mihalas D., 1978, Stellar atmospheres, second edition, W.H. Freeman and Company San Francisco
Osterbart R., Fahr H.J., 1992, A&A 264, 260
Parker E.N., 1963, Interplanatary dynamical processes, Interscience Publishers, New York, U.S.A
Ratkiewicz R., Barnes A., Molvik G.A., et al., Geophys. Res. Letters (in press)
Rottman G.J., 1988, Adv. Space Res. 8, 53
Rottman G.J., Woods T.N., White O.R., London J., 1994, The sun as a variable star: solar and stellar irradiance variations, ed. Pap J.M., Fröhlich C., Hudson H.S., Solanki S.K., Cambridge Univ. Press
Scherer H., Fahr H.J., 1995, Solar Physics 161, 383
Scherer H., Fahr H.J., 1996, A&A 309, 957
Scherer H., Fahr H.J., 1997, Solar Physics 170, 371
Soderblom D.R., 1994, Instrument Handbook for the Goddard High Resolution Spectrograph (GHRS), Version 5.0, Space Telescope Science Institute Baltimore, Maryland
Thomas G.E., 1978, Ann. Rev. Earth Planetary Sci. 6, 173
White O.R., Rottman G.J., Woods T.N., et al., 1994, JGR 99, no. A1, 369
Witte M., Rosenbauer H., Banaszkiewicz M., Fahr H., 1993, Adv. Space Res. 13,(6) 121
Wu F.M., Judge D.L., 1979, ApJ 231, 594

This article was processed by the author using Springer-Verlag LaTeX A&A style file *L-AA* version 3.